

Supplementary Information

Energy Efficient Electrochemical Reduction of CO₂ to CO Using a Three-dimensional Porphyrin/Graphene Hydrogel

Jaecheol Choi,^a Jeonghun Kim,^b Paweł Wagner,^a Sanjeev Gambhir,^a Rouhollah Jalili,^{a,e} Seoungwoo Byun,^c Sepidar Sayyar,^a Yong Min Lee,^c Douglas R. MacFarlane,^d Gordon G. Wallace,^{a,*} and David L. Officer^{a,*}

^a ARC Centre of Excellence for Electromaterials Science and the Intelligent Polymer Research Institute, Australian Institute for Innovative Materials, University of Wollongong, Wollongong, NSW, 2522, Australia

^b School of Chemical Engineering and the Australian Institute for Bioengineering and Nanotechnology (AIBN), The University of Queensland, Brisbane, QLD 4072, Australia

^c Department of Energy Science and Engineering, Daegu Gyeongbuk Institute of Science and Technology (DGIST), 333 Techno Jungang-daero, Hyeonpung-myeon, Dalseong-gun, Daegu 42988, Republic of Korea

^d ARC Centre of Excellence for Electromaterials Science, Monash University, Clayton, VIC, 3800, Australia

^e Now at Royal Melbourne Institute of Technology, Melbourne, Victoria, Australia

*E-mail: davido@uow.edu.au, gwallace@uow.edu.au

1. Supplementary figures and tables

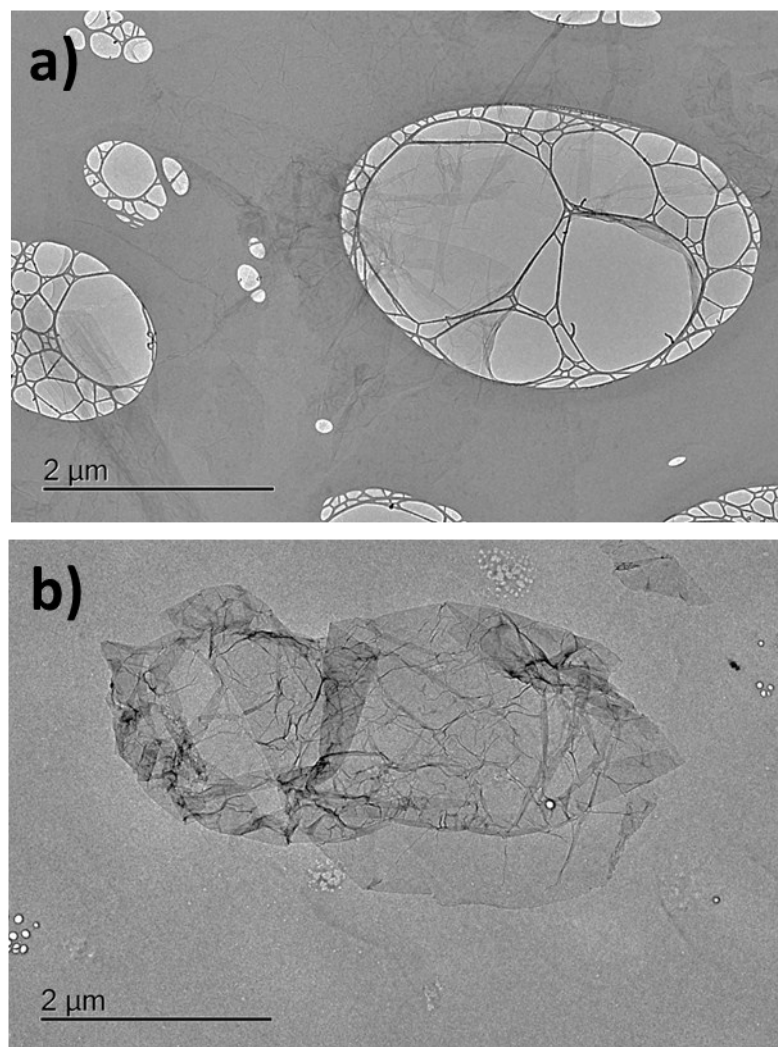


Fig. S1. TEM images of a) LCGO and b) LCGO-FeTMAP composite.

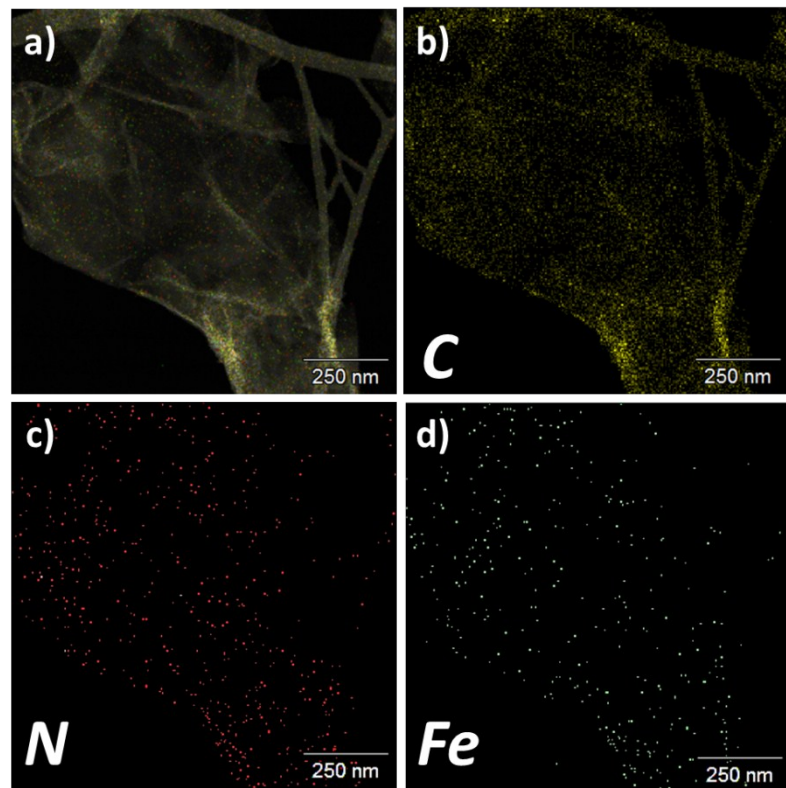


Fig. S2. EDS mapping of a) all elements, b) C, c) N and d) Fe.

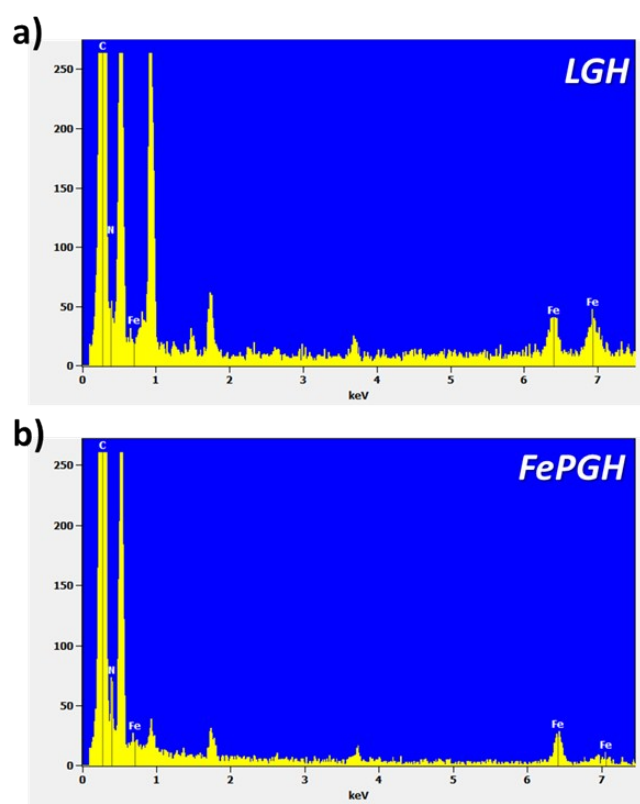


Fig. S3. EDS spectrum of a) LGH and b) FePGH.

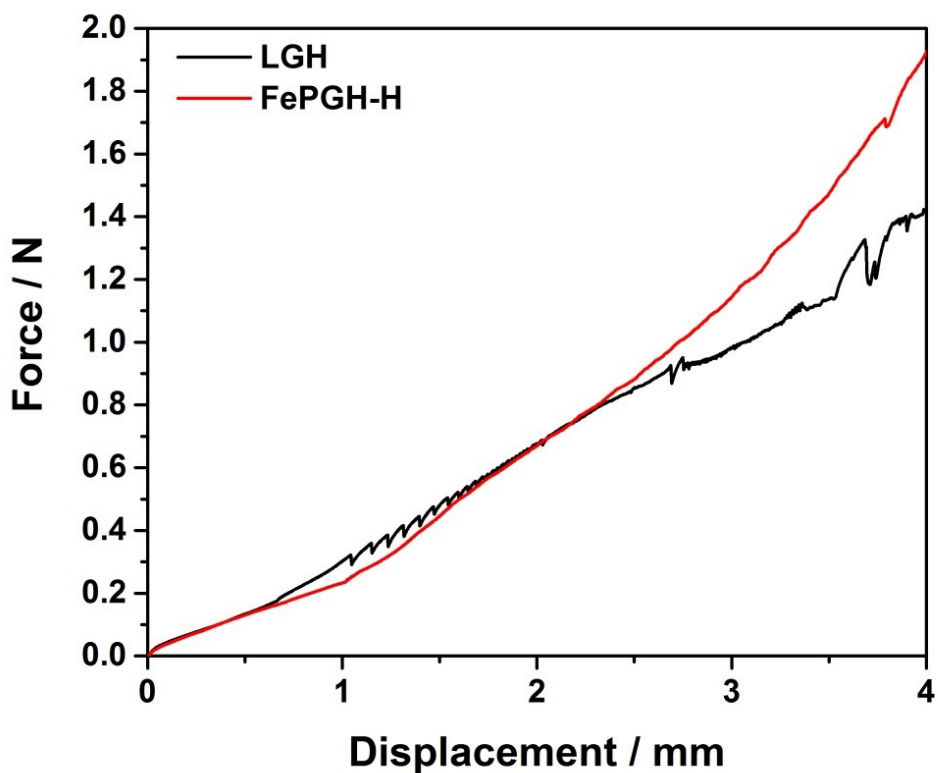


Fig. S4. Force versus displacement plots for LGH and FePGH.

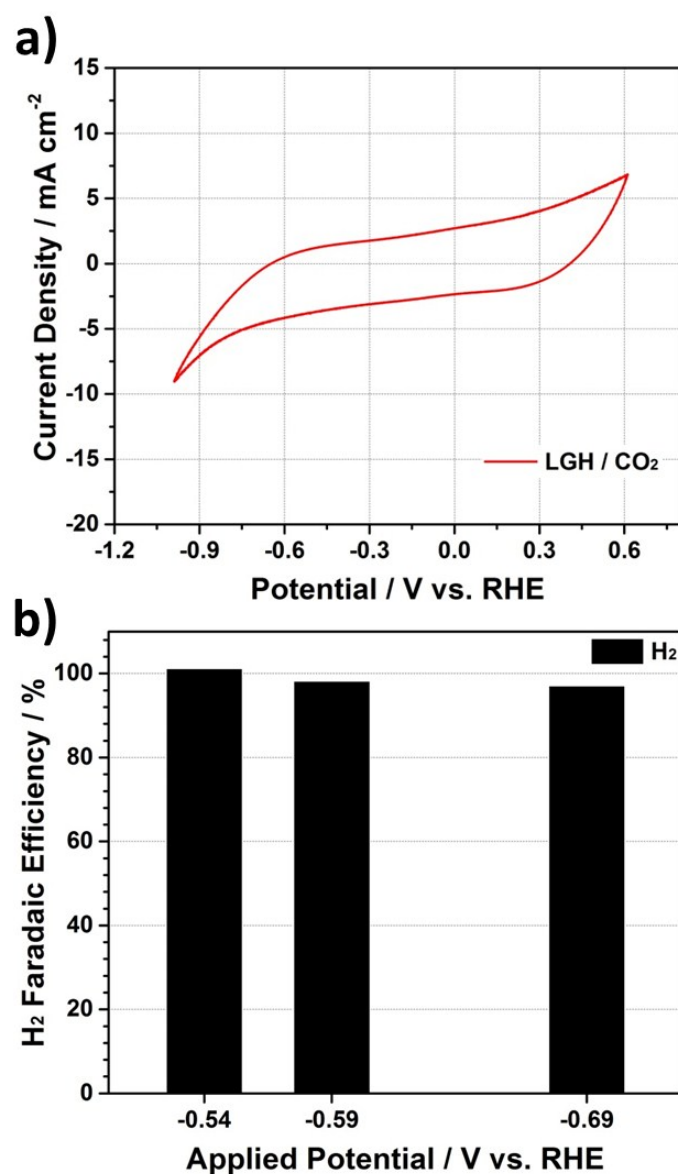


Fig. S5. Electrochemical CO_2 reduction performance of LGH. a) CV measurement of LGH electrode in a CO_2 atmosphere (scan rate: 20 mV s^{-1}). b) Gas analysis at -0.54 , -0.59 and -0.69 V.

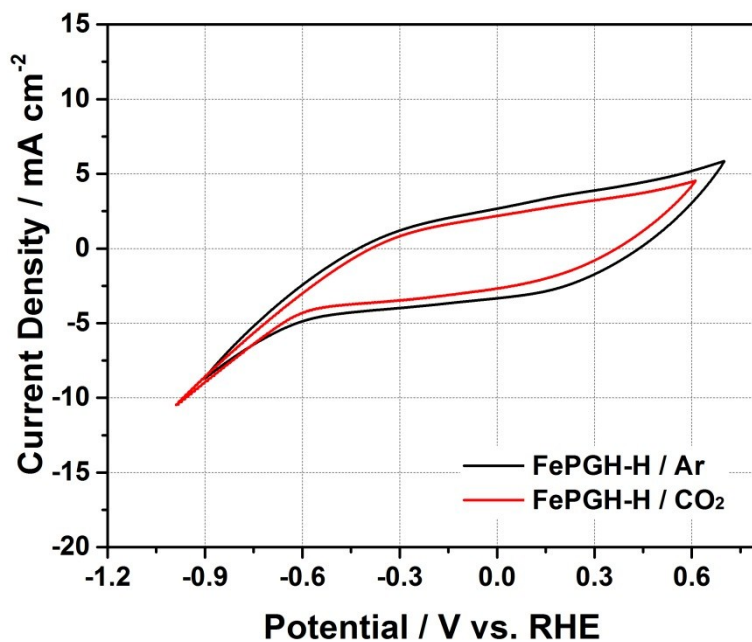


Fig. S6. Cyclic voltammogram of FePGH-H in Ar (black line) and CO₂ (red line) saturated 0.1 M KHCO₃ (scan rate: 20 mV s⁻¹).

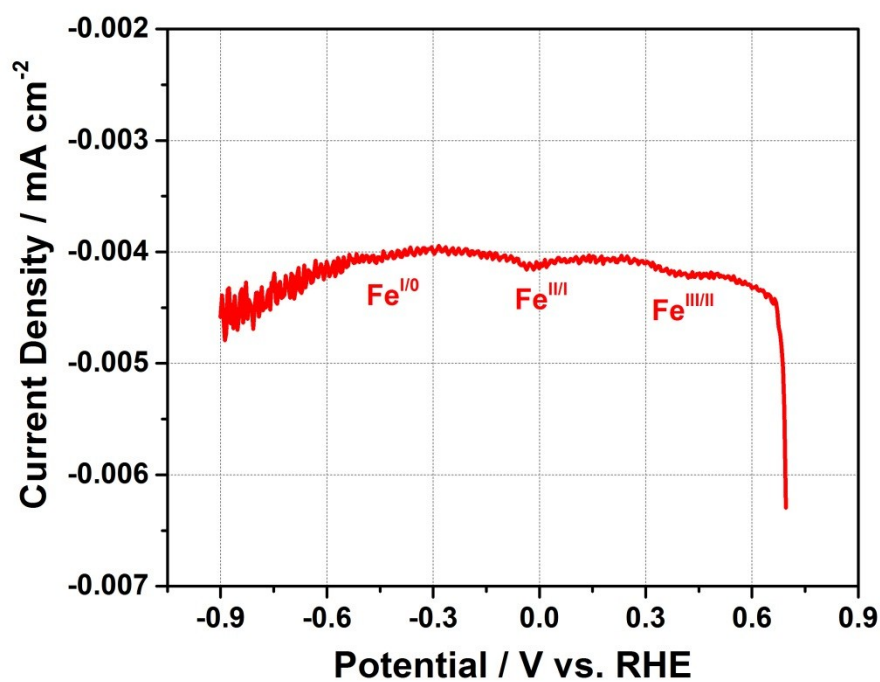


Fig. S7. DPV of FePGH-H in Ar saturated 0.1 M KHCO₃ (pH 8.3).

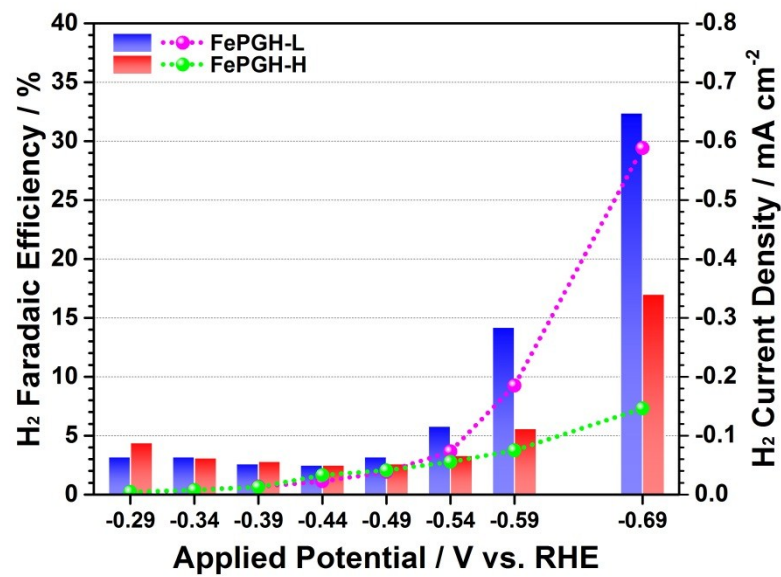


Fig. S8. H₂ FEs and H₂ partial current densities obtained by FePGH-L (blue) and -H (red).

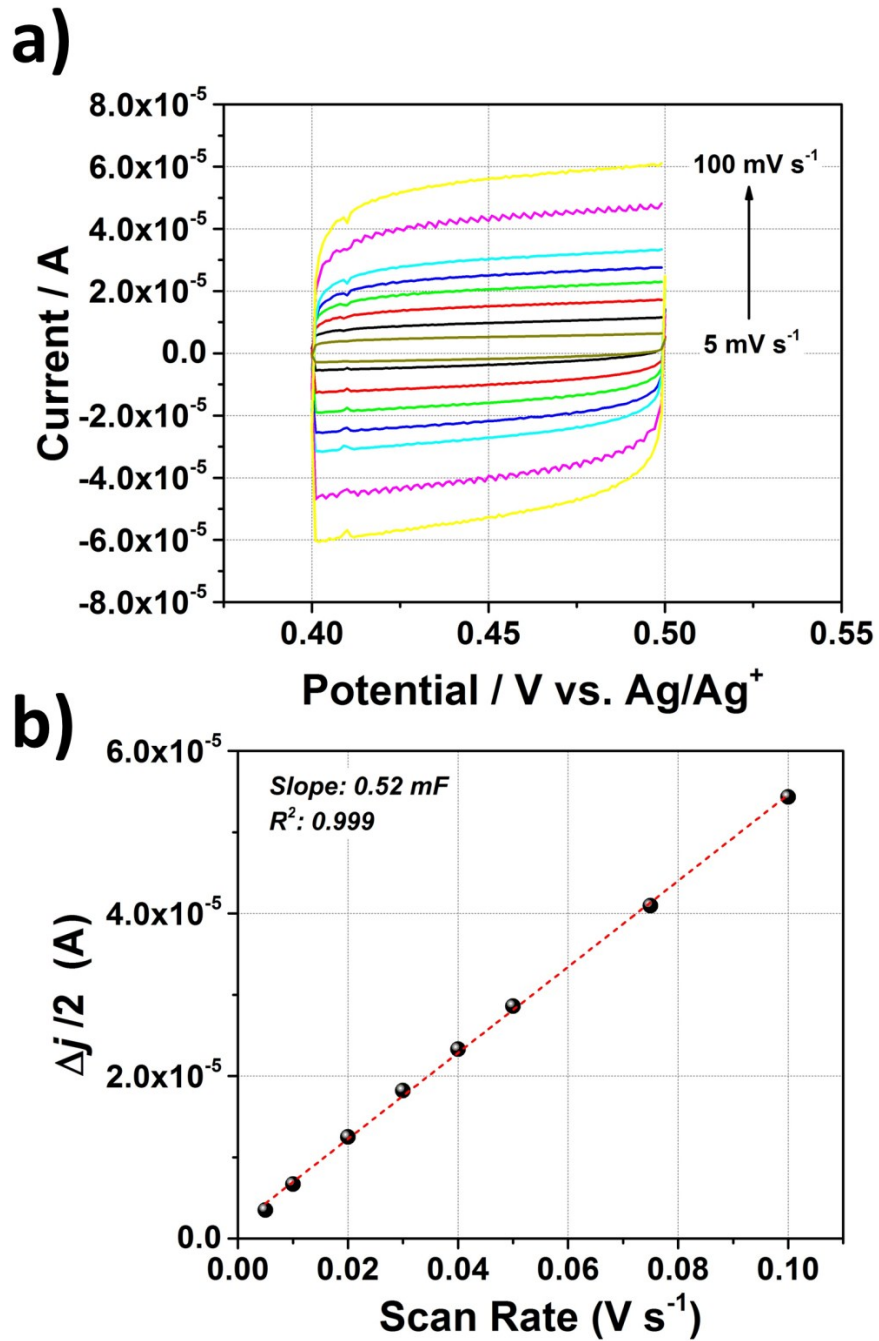


Fig. S9. Double layer capacitance measurements used for the determination of the electrochemical surface area of the RVC substrate. a) Cyclic voltammograms of the RVC electrode measured in an Ar saturated 0.1M KHCO₃ at different scan rates from 5 to 100 mV s⁻¹. b) Charging current density differences at 0.45 V against scan rates with the slope of the line giving the capacitance of the RVC electrode.

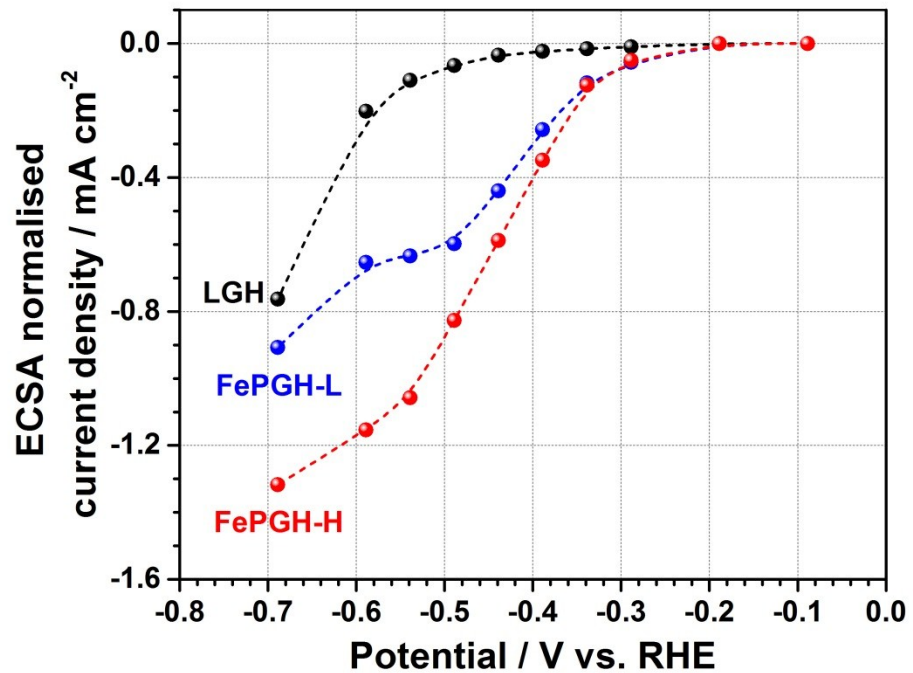


Fig. S10. ECSA-normalised current densities of LGH (black), FePGH-L (blue) and FePGH-H (red) at different applied potentials.

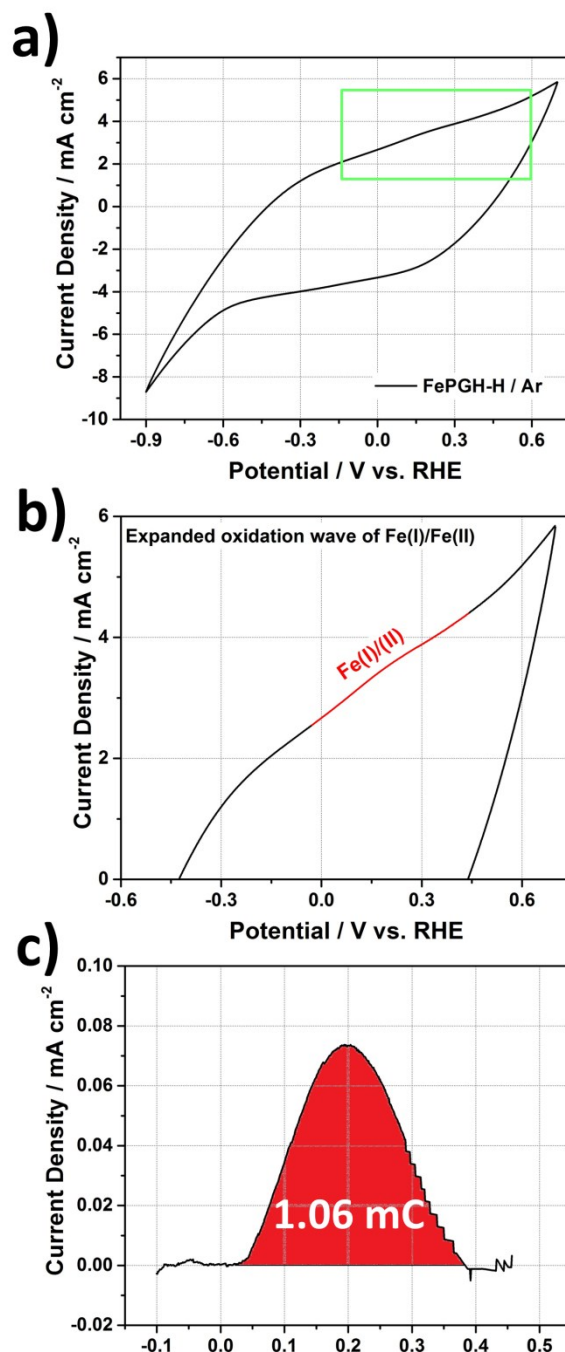


Fig. S11. a) CV of FePGH-H in Ar saturated 0.1M KHCO₃ electrolyte (pH 8.3). b) Expanded oxidation wave of Fe(I)/Fe(II) (red line). c) The total charge obtained from integration of the oxidation peak of Fe(I) to Fe(II) in a).

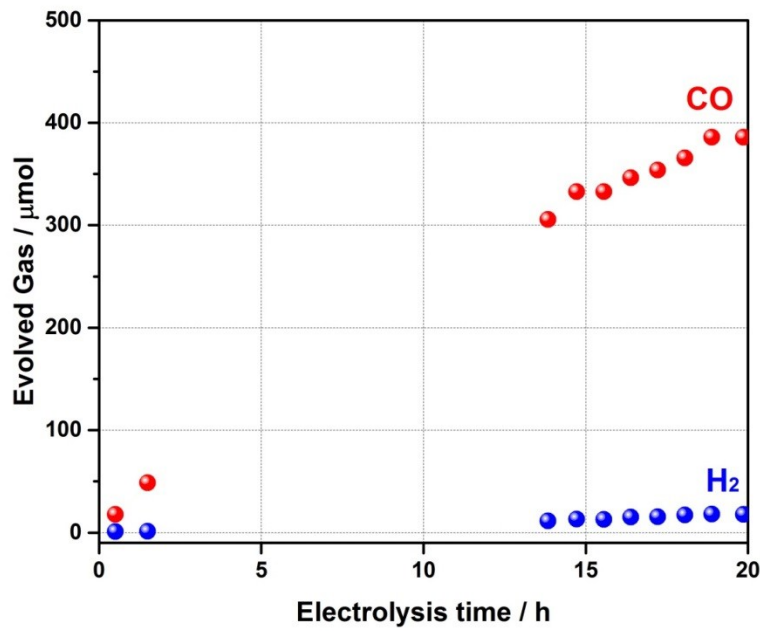


Fig. S12. Evolved CO and H₂ during 20 h electrolysis.

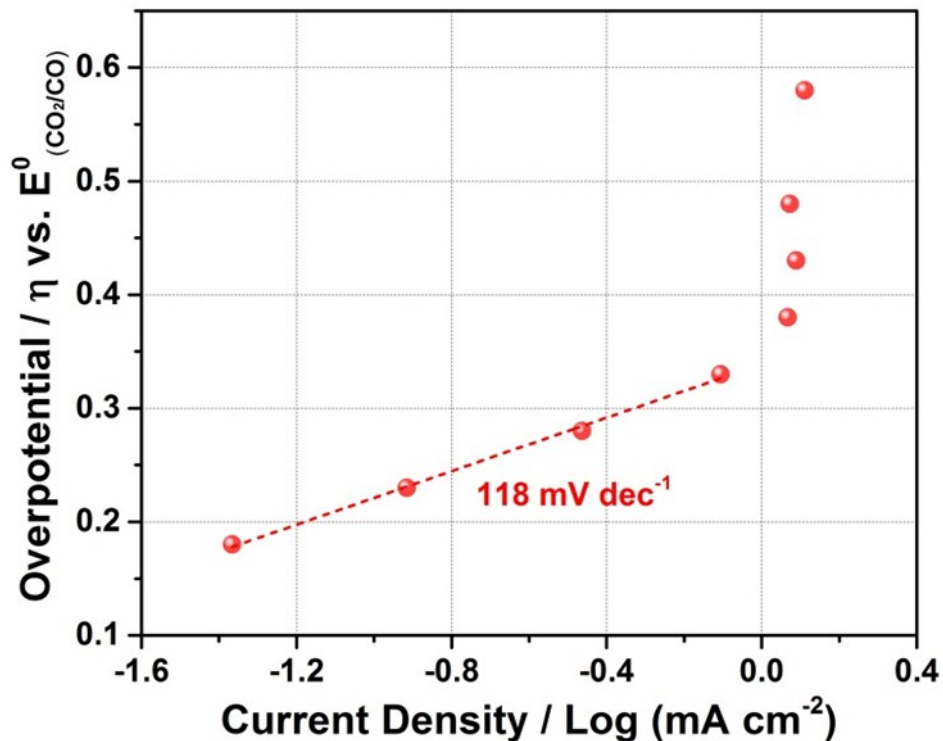


Fig. S13. Tafel plot of FePGH-H for CO production.

Table S1. Summary of the reduction potentials of FePGF and FePGH.

	Fe(III)/(II)	Fe(II)/(I)	Fe(I)/(0)
FePGF	0.13	-0.29	-0.58
FePGH	0.39	0	-0.45

Table S2. Comparison of catalysis data for FePGH prepared in this study with the state-of-the-art electrocatalysts for electrochemical CO₂ reduction to CO.

#	Catalysts (Electrolysis V vs. RHE, pH)	Active amount of molecule ($\times 10^{-9}$ mol cm $^{-2}$)	Over- potential (mV)	Current density (mA cm $^{-2}$)	Mass current density (A mg $^{-1}$)	Electro- lysis time (h)	FE CO/H ₂ (%)	TOF (s $^{-1}$)	TON	Cathodic energy efficiency (%)	Refer- ence
1	FePGH-H (-0.39V, pH 6.8)	4.23	280	~ 0.42	1.73	20	96.4% / 3.8%	0.5	37,440	79.7	This work
2	FePGH-H (-0.54V, pH 6.8)	4.23	430	~ 2.11	8.51	-	95.0% / 5.7%	2.5	-	71.9	This work
3	FePGF (-0.54V, pH 6.8)	3	430	~ 1.68	9.90	10	98.7% / 0.8%	2.9	104,400	74.7	1
4	WSCAT/Nafion /Carbon powder (-0.52V, pH 7.3)	37-74	410	~ 1.0	0.03	30	90% / 10%	0.01	1,006	68.9	2
5	CAT _{pyr} /MWCNT (-0.59V, pH 7.3)	24	480	~ 0.2	0.14	3	93% / 4%	0.04	432	68.5	3
6	CAT _{CO2H} /MWCNT (-0.62V, pH 7.3)	64	510	~ 0.16	0.36	3	80% / n.a.	0.1	1,080	57.9	4
7	CoPc/MWCNT (2.5%) (-0.63V, pH 6.8)	18	520	~ 10	8.67	10	92% / 6.4%	2.6	93,600	66.3	5
8	CoPc-CN/MWCNT (3.5%) (-0.46V, pH 7.2)	18	350	~ 5.6	4.65	-	88% / 13%	1.4	-	69.8	5
9	CoPc-CN/MWCNT (3.5%) (-0.63V, pH 7.2)	18	520	~ 15	13.86	-	98% / 3.3%	4.1	-	70.6	5
10	CoTPP/SWCNT (-0.68V, pH 7.2)	170	570	~ 3.2	0.27	4	85% / 9%	0.08	1,194	59.6	6
11	CoPPc/CNT (-0.54V, pH 7.4)	6.4	430	~ 12	0.39	24	80-90% / n.a.	1.65	142,716	64.4	7
12	CoPc-P4VP (-0.73V, pH 4.7)	1.3	620	~ 2	23.10	2	89% / 5%	4.8	34,560	60.8	8
13	CoFPC (-0.80V, pH 7.2)	13	690	~ 4.5	5.46	2	93% / 5%	1.61	11,592	61.4	9
14	COF-367-Co (1%) (-0.67V, pH 7.3)	2.0	560	~ 0.45	2.02	8	53% / 62%	0.62	17,856	37.4	10
15	Fe-PB (-0.63V, pH 7.3)	2.26	520	~ 0.53	3.58	24	85% / 15%	0.64	32,770	61.2	11

2. References

1. J. Choi, P. Wagner, R. Jalili, J. Kim, D. R. MacFarlane, G. G. Wallace and D. L. Officer, *Adv. Energy Mater.*, 2018, **8**, 1801280.
2. A. Tatin, C. Comminges, B. Kokoh, C. Costentin, M. Robert and J.-M. Savéant, *Proc. Natl. Acad. Sci. U.S.A.*, 2016, **113**, 5526-5529.
3. A. Maurin and M. Robert, *J. Am. Chem. Soc.*, 2016, **138**, 2492-2495.
4. A. Maurin and M. Robert, *Chem. Commun.*, 2016, **52**, 12084-12087.
5. X. Zhang, Z. Wu, X. Zhang, L. Li, Y. Li, H. Xu, X. Li, X. Yu, Z. Zhang and Y. Liang, *Nature Commun.*, 2017, **8**, 14675.
6. X. M. Hu, M. H. Rønne, S. U. Pedersen, T. Skrydstrup and K. Daasbjerg, *Angew. Chem., Int. Ed.*, 2017, **56**, 6468-6472.
7. N. Han, Y. Wang, L. Ma, J. Wen, J. Li, H. Zheng, K. Nie, X. Wang, F. Zhao and Y. Li, *Chem*, 2017, **3**, 652-664.
8. W. Kramer and C. McCrory, *Chem. Sci.*, 2016, **7**, 2506-2515.
9. N. Morlanés, K. Takanabe and V. Rodionov, *ACS Catal.*, 2016, **6**, 3092-3095.
10. S. Lin, C. S. Diercks, Y.-B. Zhang, N. Kornienko, E. M. Nichols, Y. Zhao, A. R. Paris, D. Kim, P. Yang and O. M. Yaghi, *Science*, 2015, **349**, 1208-1213.
11. P. T. Smith, B. P. Benke, Z. Cao, Y. Kim, E. M. Nichols, K. Kim and C. J. Chang, *Angew. Chem., Int. Ed.*, 2018.